ACS APPLIED NANO MATERIALS
Cite This: ACS Appl. Nano Mater. 2019, 2, 5587−5593
Article
www.acsanm.org

Multimodal Magneto-Fluorescent Nanosensor for Rapid and Specific Detection of Blood-Borne Pathogens

Tuhina Banerjee,* Tanuja Tummala, Rebekah Elliott, Vedant Jain, Wesley Brantley, Laci Hadorn, and Santimukul Santra*

Department of Chemistry, Pittsburg State University, 1701 South Broadway Street, Pittsburg, Kansas 66762, United States

Supporting Information

ABSTRACT: Detection of bacterial contaminants in blood and platelet concentrates (PCs) continues to be challenging in clinical settings despite available current testing methods. At the same time, it is important to detect the low bacterial contaminants present at the time of transfusion. Herein, we report the design and synthesis of a dual-modal magneto-fluorescent nanosensor (MFnS) by integrating magnetic relaxation and fluorescence modalities for the wide-range detection of blood-borne pathogens. In this study, functional MFnSs are designed to specifically detect *Staphylococcus epidermidis* and *Escherichia coli*, two of the predominant bacterial contaminants of PCs. Specific interaction between the target pathogen and functional MFnS resulted in the change of water proton's magnetic relaxation time, indicative of sensitive detection of the target bacteria from low to high colony-forming units (CFUs). In addition, the acquired magnetic relaxation signal of the MFnS further facilitated quantitative assessment of the slow and fast growth kinetics of target pathogens. Moreover, the presence of fluorescence modality in MFnS allowed for the detection of multicontaminants. Bacterial detection was also performed in complex media including whole blood and PCs, which further demonstrated its robust detection sensitivity. Overall, our study indicated that the designer MFnS will have potential for the wide-range detection of blood-borne pathogens and features desirable qualities including timeliness, sensitivity, and specificity.

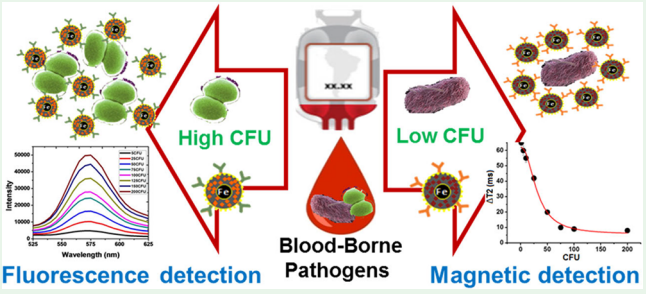

KEYWORDS: *magneto-fluorescent nanosensors, blood-borne pathogen, magnetic relaxation, fluorescence, sepsis*

INTRODUCTION

Bacterial contamination of blood and blood products, particularly platelet concentrates (PCs), continues to pose a major challenge in the world of transfusion medicine.[1−4] This, in turn, often leads to various life-threatening medical conditions including sepsis. According to Centers for Disease Control and Prevention estimates, 1 in 1000 platelet units may be contaminated with bacteria at the time of transfusion.[5] Additionally, the frequency of bacterial contamination in transfused PCs is 10 times higher than that in red blood cells.[5] *Staphylococcus epidermidis* (S.e.), *Staphylococcus aureus* (S.a.), *Escherichia coli* (E.c.), and *Bacillus cereus* (B.c.) are the most frequent bacteria found in contaminated PCs.[6,7] However, the storage temperatures and agitation necessary to maintain the function of plasma concentrates, on the other hand, contribute significantly to the bacterial growth within the storage temperatures ranging from 20 to 25 °C.[6]

Currently, several methods are available for the screening of PCs for bacterial contaminants. For example, culture-based testing, real-time polymerase chain reaction (PCR), and flow cytometry (FCM) are commonly used techniques. While these methods are sensitive, they carry their own limitations and may not completely meet the required standard for detection.[8−14] In particular, the culture-based testing method is one of the most commonly used techniques for bacterial detection. Although this method is inexpensive, it is extremely inefficient with regard to time and labor. The real-time PCR is often prone to false-positive results because of DNA contamination of the PCR reagents.[12,13] FCM is also used for the detection of PC contaminations. While effective, several modifications including culturing of PCs in bacterial growth media are needed for low concentration levels of bacteria in platelets, which limits the detection capability.[11−19] Other obstacles for FCM include slow-growing bacteria not reaching titers at high enough levels to be detected because of differential growth kinetics. Some of these methods are also used for the testing of blood cultures for bloodstream infection detection.[11,12,15,16] Hence, new technologies are arguably needed that can detect pathogens in simple and complex media with minimal sample preparation, without the need for further sample amplification, and with low turnaround time.

In recent years, the unique combination of nanotechnology and magnetic relaxation (MR) achieved through the fabrication of magnetic relaxation nanosensors (MRnSs) has

Received: June 17, 2019
Accepted: August 19, 2019
Published: August 19, 2019

DOI: 10.1021/acsanm.9b01158
ACS Appl. Nano Mater. 2019, 2, 5587−5593

been extensively used for the rapid detection of bacterial targets with greater sensitivity.[20−26] These MRnSs are synthesized by conjugating antibodies/affinity ligands on the surface of a superparamagnetic iron oxide nanoparticle (IONP). The underlying principle behind the detection lies in the switching of MRnSs between dispersed and clustered states due to interaction with the targeted bacterial contaminants, which results in a simultaneous change in the spin−spin relaxation time (T_2 MR) of the water protons.

Moreover, the magnitude of ΔT_2 MR can be directly correlated with the target concentration. In likewise fashion, the use of magnetic nanoparticles in conjunction with fluorescence technology leads to significant improvements in the detection of pathogens at high concentrations, hence allowing a wide detection range. In our previous findings, the integration of MR technology with fluorescence allowed the rapid and sensitive detection of low and high concentrations of *E. coli* O157:H7 [1−100 colony-forming units (CFUs)/mL] in water and liquid food samples.[25,26]

In this study, we have designed new MFnS for the rapid and specific detection of various blood-borne pathogens. These functional MFnSs (Figure 1) are also suitable for the simultaneous detection of multicontaminants in PCs and in whole blood. *S. epidermidis* was chosen as one of the target pathogens for the present study because it accounts for 25% of bacterial contaminations in PCs.[8−10] On the other hand, *E. coli* was selected because of its faster growth rate than *S. epidermidis*,[2] in order to evaluate the differential growth kinetics in one step using our designer MFnS. Overall, the present work represents novel multimodal MFnS nanoplatforms for the rapid, sensitive, and differential detection of multiple pathogens in simple and complex media.

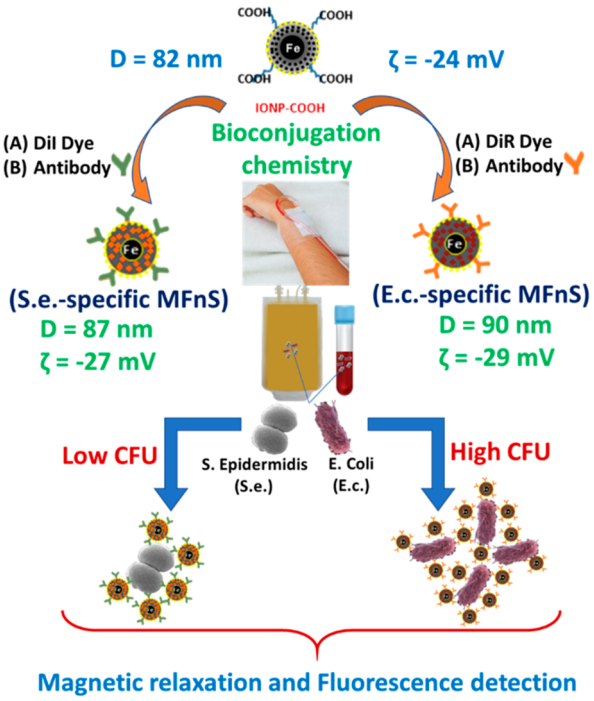

Figure 1. Schematic representation of the mechanism of dual-mode detection of bacterial contamination in whole blood and PCs using functional MFnSs.

MATERIALS AND METHODS

Materials. ACS reagent grade iron salts [ferric chloride ($FeCl_3 \cdot 6H_2O$) and ferrous chloride ($FeCl_2 \cdot 4H_2O$)], hydrochloric acid, and ammonium hydroxide were purchased from Fisher Scientific. Poly(acrylic acid) (PAA), 2-morpholinoethanesulfonic acid (MES), 1-ethyl-3-[3-(dimethylamino)propyl]carbodiimide hydrochloride (EDC), and *N*-hydroxysuccinimide (NHS) were purchased from Sigma-Aldrich and used as received. Bacterial strain *S. epidermidis* and *E. coli* were acquired from American Type Culture Collection (ATCC). *S. epidermidis* monoclonal antibody (MA1-35788) was purchased from Invitrogen, and *E. coli* monoclonal (ab25823) was obtained from Abcam. Nutrient broth and nutrient agar were purchased from Becton Dickinson. The fluid thioglycolate medium was procured from BBL. Human PC and whole human blood were purchased from Becton Dickinson.

Synthesis and Purification of Functional MFnS. *Encapsulation of Fluorescent Dyes in PAA-Coated IONPs (IONP-COOHs).* First, IONP-COOH was synthesized according to our previously reported[27] method and briefly described in Scheme S1. Fluorescent DiI/DiR dyes were encapsulated within the PAA coatings of IONPs using a solvent diffusion method. Briefly, 2.0 μL of a DiI/DiR dye (3.0 mmol) reconstituted in 100 μL of dimethyl sulfoxide was added in a dropwise manner to 4.0 mL of IONP-COOH (4.0 mmol) with constant mixing at 1100 rpm. Finally, the resulting IONP-DiI-COOH and IONP-DiR-COOH solutions were purified using a magnetic column with phosphate-buffered saline (PBS; pH 7.4; final concentration [Fe] = 3.0 mmol) as the eluent and a QuadroMAX LS column from Miltenyibiotec. Dynamic light scattering (DLS; Figure S1) and UV−vis (Figure 2) studies further confirmed the successful encapsulation of the dyes within the PAA coatings of the IONPs.

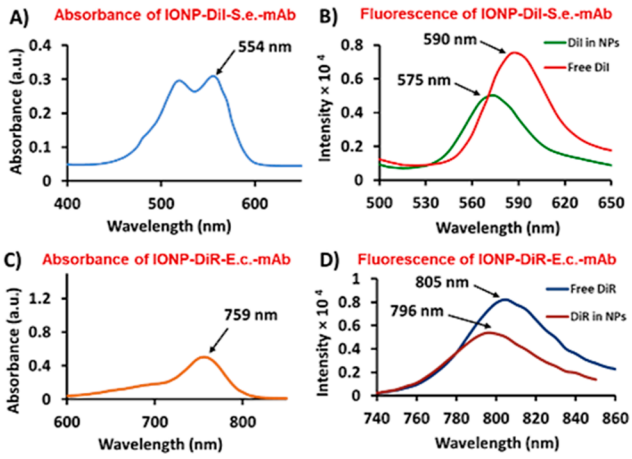

Figure 2. Spectrophotometric characterization of IONP-DiI-S.e.-mAb (MFnS-S.e.; A and B) and IONP-DiR-E.c.-mAb (MFnS-E.c.; C and D) MFnSs (2.0 mmol). The successful entrapment of fluorescent dyes into MFnSs was confirmed by collecting noticeable blue-shift fluorescent signals (B and D) from the corresponding free dyes.

Formulation of Antibody-Conjugating MFnSs. Antibody-conjugating magnetic nanoparticles were synthesized following our previously reported protocol.[24−26] Briefly, the following solutions were prepared: (1) 4.0 mL of IONP-DiI/DiR-COOH (3.0 mmol) added to 1 mL of PBS (pH 7.4); (2) 5.0 mg of EDC in 250 μL of a MES buffer (0.1 M, pH 6.0); (3) 3.0 mg of NHS in 250 μL of a MES buffer (0.1 M, pH 6.0); (4) 5.0 μg of the corresponding antibodies IgG, the *S. epidermidis* mAb, or *E. coli* mAb in 225 μL of PBS (pH 7.4). After the preparation of solution 2, it was immediately added to solution 1, followed by the addition of solution 3, with brief mixing. This reaction mixture was incubated for an additional 3 min, and the final addition of solution 4 was done in a dropwise manner. The antibody-conjugated nanoparticles (MFnS-S.e., IONP-DiI-S.e.-mAb;

DOI: 10.1021/acsanm.9b01158
ACS Appl. Nano Mater. 2019, 2, 5587−5593

MFnS-E.c., IONP-DiR-E.c.-mAb) were kept in a table mixer at room temperature for 3 h and then incubated at 4 °C overnight. After conjugation, further purification was performed using a QuadroMACS magnetic column (LS) to separate the unconjugated antibodies and other free reagents. The final concentration of the antibody-conjugating MFnSs was adjusted to [Fe] = 2.0 mmol.

Characterizations of the Functional MFnS. *Size, ζ Potential, Fluorescence, and MR Measurements.* Using Malvern's Nano-ZS90 Zetasizer, we measured the average size and overall surface charge (ζ potential) of the IONP-COOH and MFnS encapsulated with two different fluorescent dyes. For average size measurements, three consecutive measurements were taken from a sample, whereas one measurement was taken per sample for collecting the ζ potential. The average size and ζ potential of IONP-COOH were found to be 82 ± 1 nm and −24 mV, respectively (Figure 1). The average size and surface charge of IONP-DiI-mAb (MFnS-S.e.) were 87 ± 2 nm and −27 mV, respectively. For IONP-DiR-mAb (MFnS-E.c.), the average size and surface ζ potential were found to be 90 ± 1 nm and −29 mV, respectively (Figure S2). Using TECAN's infinite M200 PRO high-throughput plate reader, the UV−vis and fluorescence of MFnS-S.e. and MFnS-E.c. were measured. Fluorescence experiments showed emission at 575 and 796 nm for MFnS-S.e. and MFnS-E.c., respectively, which confirmed the effective encapsulation of both dyes (Figure 2). Bruker's magnetic relaxometer mq20 (0.47T, B = 20 MHz) was used for spin−spin T_2 MR experiments and showed T_2 MR at 152 and 165 ms for MFnS-S.e. and MFnS-E.c., respectively (Figure S3), treated as baselines for all detection experiments.

Bacterial Culture. The lyophilized pellet of bacteria obtained from ATCC was resuspended in 1.0 mL of nutrient broth. To the 1.0 mL of the bacterial suspension was added 5.0 mL of fresh media. A total of 100 μL of this solution was streaked on an agar plate and incubated for 24 h at 37 °C. After 24 h, colonies were observed on the plates (Figure S3). An isolated bacterial colony was selected and cultured in 15 mL of nutrient broth at 37 °C until the desired optical density (OD) of 0.2 at 600 nm was obtained followed by serial dilutions.[25] The final CFU count was confirmed using the gold standard plate counting method.

Detection of Bacterial Contamination in Complex Media Using MR Technology. All T_2 MR measurements were performed at 37 °C using Bruker's magnetic relaxometer. A constant amount of MFnS (200 μL, [Fe] = 2.0 mmol) was added to PBS solutions (500 μL, 1X, pH 7.4) spiked with increasing concentrations (ranging from 1 to 200 CFUs/mL) and incubated at 37 °C for 15 min, before these individual solutions were transferred to the magnetic relaxometer. For all of the individual readings, the corresponding baseline value was measured containing only PBS (500 μL) and MFnS (200 μL, [Fe] = 2.0 mmol). A similar protocol was repeated when the T_2 MR readings were measured in complex media including whole blood and PC. For growth kinetic experiments, 400 μL of PC was added to 400 μL of the bacterial growth medium (BBL fluid thioglycollate medium) with the final concentration of spiked bacteria adjusted to 10 CFUs/mL. To this solution was added 200 μL of antibody-conjugating MFnS ([Fe] = 2.0 mmol), and the resulting mixture was incubated at 37 °C for 48 h. To assess the growth kinetics, the MR data (ΔT_2) were collected every 4 h. At every time point, the baseline ($T_{2,\mathrm{initial}}$) was also recorded for the ΔT_2 calculations ($\Delta T_2 = T_{2,\mathrm{final}} - T_{2,\mathrm{initial}}$), which represents the true changes in the MR for each experiment.

Detection of Bacterial Contamination in Complex Media by Fluorescence Measurements. After collection of the MR data, the samples were centrifuged at 2880*g* for 10 min to remove any unbound nanosensors. To the remaining bacterial cell pellet was added 100 μL of 1X PBS (pH 7.4), and the pellet was resuspended. From this suspension, 70 μL of the sample was taken and added to a well of a 96-well plate for measurement of the fluorescence intensity using a plate reader. Samples corresponding to a mixture of two bacterial contaminants were prepared by adding equal amounts of CFUs of both bacteria in 200 μL of PC, followed by the addition of equimolar amounts of antibody-conjugated nanosensors (200 μL, [Fe] = 2.0 mmol). Mixed solutions were then incubated for 15 min at 37 °C. After incubation in a fashion similar to that mentioned above, MR and fluorescence measurements were performed. The fluorescence data from the experiments in the whole blood sample were interfered with by the residual blood components.

Data Analysis. All of the plots in the manuscripts were generated using *OriginPro 8.0*. The average of three independent experiments was reported. Moreover, for each experimental condition, measurements were done in triplicate. For the MR measurements, the best model curve was acquired using a sigmoidal fit.

■ RESULTS AND DISCUSSION

Bacterial Pathogen Detection Using a Dual-Modal Functional MFnS. To achieve sensitive and multiplex detection of pathogens, functional MFnSs were designed and synthesized as shown in Figure 1. In this study, surface modification on MFnS allowed us to specifically detect blood-borne bacterial pathogens. Moreover, the addition of fluorescence modality enabled wide-range detection and discrimination between different bacteria.

Toward this goal, IONP-COOHs were formulated according to the previously reported solvent precipitation method (Scheme S1).[27] Following the synthesis, fluorescent dyes were encapsulated within the PAA coatings of IONPs. The resuspended IONP-DiI-COOH ([Fe] = 3.0 mmol) showed a diameter of 84 ± 2 nm and a surface charge of −25 mV. The DiR-encapsulating IONPs (IONP-DiR-COOH; [Fe] = 3.0 mmol) reported a diameter of 85 ± 1 nm and contained a charge of −25 mV (Figure S1). These fluorescent-labeled IONPs were found to be stable for an extended period of time (Table S1). Next, monoclonal IgG1 antibodies specific for *S. epidermidis* (anti-S.e.-mAb) and *E. coli* (anti-E.c.-mAb) were conjugated on the IONP's surface using water-based carbodiimide (EDC/NHS) chemistry. Detailed characterization studies including the size and ζ potential were carried out and are shown in Figure S2. The resuspended IONP-DiI-S.e.-mAb ([Fe] = 2.0 mmol) showed a diameter of 87 ± 2 nm and a surface charge of −27 mV. IONP-DiR-E.c.-mAb ([Fe] = 2.0 mmol) reported a diameter of 90 ± 1 nm and contained a charge of −29 mV. As shown, dispersed MFnSs were synthesized with an increase in the overall size after conjugation with antibodies. These functional MFnSs were found to be stable for a longer period of time not only in PBS (1X, pH 7.4) but also in 10% whole blood and in serum (Figure S4), as determined by DLS measurements over a period of 2 months. Spectrophotometric studies showed an absorption band at λ_{abs} = 554 nm and an emission band at λ_{em} = 575 nm for IONP-DiI-S.e.-mAb and an absorption band at λ_{abs} = 759 nm and an emission band at λ_{em} = 796 nm for IONP-DiR-S.e.-mAb (Figure 2). The emission spectra were compared with those of the corresponding free optical dyes, indicating that the synthesized MFnSs were not contaminated with any free optical dyes after purification using a magnetic column. These results were further confirmed for the successful encapsulation of fluorescent dyes within the PAA coatings of MFnSs.

Next, for the dual-modal (T_2 MR and fluorescence) detection of pathogens, the following steps were followed. The purified antibody functional MFnS (200 μL, [Fe] = 2 mmol) was incubated for 15 min with bacterial solutions (500 μL) from low to high concentrations (1−200 CFUs/mL), and the sensitive T_2 MR readings were collected in each case. Following the collection of T_2 readings, the solutions were centrifuged at 2880*g* for 10 min to remove any unbound MFnSs. The remaining MFnS-bound bacterial cell pellets were

DOI: 10.1021/acsanm.9b01158
ACS Appl. Nano Mater. 2019, 2, 5587−5593

resuspended in PBS, and the corresponding fluorescence measurements were recorded. According to our hypothesis, when Ab-MFnSs are placed in a solution with bacterial colonies, they migrate around the bacteria's outer membrane via specific interactions between the surface functional IgG1 Ab and bacterial epitope. Because of this binding and clustering of the nanosensors around the bacterial colonies, interaction between the magnetic nanosensors and their surrounding water protons is inhibited, which results in a change in the spin−spin MR time (T_2 ms). In the presence of a small amount of bacteria (low concentration), binding of MFnS results in a higher ΔT_2 value. As the concentration is raised, the nanosensors disperse within a given voxel because of the presence of additional bacterial CFUs. This phenomenon results in a reduced ΔT_2 value, demonstrating that detection via MR is highly sensitive for low counts of target pathogens.

In our initial set of experiments, MFnS-based detections were evaluated using *S. epidermidis* and *E. coli*, which were cultured in nutrient broth (Figure S3A,B) and serially diluted in PBS (1X, pH 7.4) with increasing concentrations (CFU counts confirmed by plate counting). Each diluted solution (500 μL) was incubated for 15 min with the corresponding Ab-MFnS (200 μL, [Fe] = 2 mmol) at 37 °C and then transferred to a magnetic relaxometer (B = 0.47T) for collection of the ΔT_2 values. Baseline T_2 MR values for both Ab-MFnSs were collected using PBS with no bacterial colonies (Figure S3) for the calculation of ΔT_2. As shown in Figure 3A,

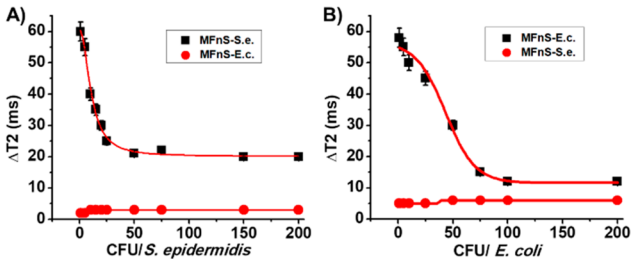

Figure 3. (A) *S. epidermidis* and (B) *E. coli* cultured in nutrient broth serially diluted in PBS (1X, pH 7.4) with increasing concentrations (1−200 CFUs/mL). Each bacterial solution (500 μL) was incubated for 15 min with a specific Ab-MFnS (200 μL, [Fe] = 2 mmol) at 37 °C before collection of the ΔT_2 values. Specificity testing was conducted using anti-S.e.-mAb-conjugated IONPs (MFnS-S.e.) in the presence of 10 CFUs of *E. coli*. This resulted in little to no binding (●, Figure 3A) compared to the 10 CFUs of *S. epidermidis* with ΔT_2 = 55 ms. Similar specificity experiments were performed for *S. epidermidis* (●, Figure 3B). Each experiment was performed in triplicate, and the data are represented as mean ± standard deviation errors.

dose-dependent significant T_2 changes were observed at low concentrations for *S. epidermidis* (linearity plot of the MR data; Figure S5) and for *E. coli* (Figure 3B). Results indicated that the MR detection modality is less sensitive for differentiating between two high-concentration solutions ($\Delta T_{2,\ 50\ \mathrm{CFU}}$ = 19 ms and $\Delta T_{2,\ 200\ \mathrm{CFU}}$ = 20 ms; Figure 3A). As a result, it was vital to pair this MR modality with the fluorescence detection modality to discriminate between two high-concentration solutions of pathogens. To address these detection limitations at higher concentrations after the T_2 measurements, the corresponding fluorescence data were collected from the MR samples using a high-throughput plate reader. To accomplish this, the bacterial solutions were removed from the relaxometer and then centrifuged at 2880*g* for 10 min to remove any unbound nanosensors. The remaining bacterial cell pellet was then resuspended in 100 μL of PBS (1X, pH 7.4). Each of these samples (80 μL) was added to a 96-well plate, and the fluorescence intensities from the samples were recorded. The fluorescence results (Figure 4A,B) showed a linear increase in

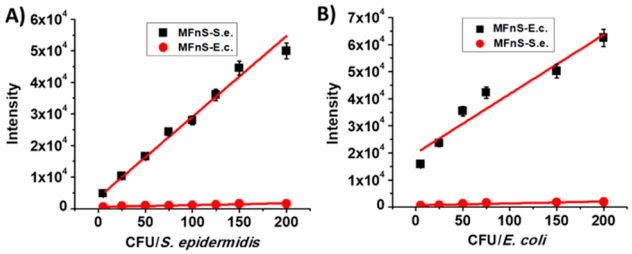

Figure 4. Detection of (A) *S. epidermidis* and (B) *E. coli* by using the fluorescence modality. MFnS-bound bacterial solutions were centrifuged and resuspended in the bacterial cell pellets in PBS (1X, pH 7.4) before the fluorescence measurements were taken. The specificity testing was conducted using anti-S.e.-mAb-conjugated IONPs (MFnS-S.e.) in the presence of *E. coli*, which resulted in little to no binding (●, Figure 4A). Similar specificity experiments were performed for *S. epidermidis* (●, Figure 4B). Each experiment was performed in triplicate, and the data are represented as mean ± standard deviation errors.

the emission intensity (linearity plot of fluorescence; Figure S6) at higher concentrations, where more MFnSs are available to bind with increased bacterial colonies, leading to amplified fluorescence signals from the encapsulating optical dye molecules in MFnS. This dual-modal detection modality would increase the sensitivity and accuracy for both high- and low-concentration solutions. Separate sets of experiments were carried out to assess the specificity in pathogen detection using our customized Ab-MFnS. Anti-S.e.-mAb-conjugated IONPs (MFnS-S.e.; 200 μL, [Fe] = 2 mmol) were mixed with 500 μL of 1X PBS (pH 7.4) containing 10 CFUs of *E. coli*. This resulted in little to no change in the ΔT_2 MR signal (●, Figure 3A). However, when this experiment was carried out in the presence of 10 CFUs of *S. epidermidis*, a sharp change in ΔT_2 MR = 55 ms was recorded. Similar specificity experiments were performed for *S. epidermidis* detection using anti-E.c.-mAb-conjugated IONPs (●, Figure 3B). As expected, the fluorescence experiments showed minimum binding in these control experiments (●, Figure 4A,B). These results indicated the specific pathogen detection capabilities of our functional Ab-MFnS. Taken together, the above experiments indicated that specific detection by MR is more efficient for low bacterial concentrations, whereas fluorescence-based detection is more accurate for higher CFUs.

Rapid and Sensitive Detection of Pathogens Using MFnSs. In order to demonstrate the faster detection capability and sensitivity of the formulated MFnS, time-dependent assays were performed for *S. epidermidis* and *E. coli*, separately. Samples were prepared by mixing 500 μL of 1X PBS spiked with 2 CFUs/mL of *S. epidermidis*/*E. coli* and 200 μL of specific Ab-MFnS ([Fe] = 2 mmol) at 37 °C. The T_2 MR data were collected at different time points over a period of 15 min (Figure 5). The results showed our MFnS was able to detect specific pathogen within 2 min of incubation. Minimal variation between the ΔT_2 values over 15 min for either

DOI: 10.1021/acsanm.9b01158
ACS Appl. Nano Mater. 2019, 2, 5587−5593

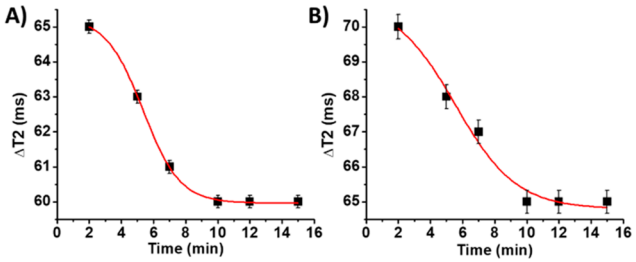

Figure 5. Time-dependent MR assays for (A) *S. epidermidis* and (B) *E. coli* performed to demonstrate the sensitivity of magnetic nanosensor and pathogen interactions. Each experiment was performed in triplicate, and the data are represented as mean ± standard deviation errors.

pathogen further proves the sensitivity in pathogen detection of our functional MFnS.

Rapid Pathogen Detection in Blood and PC Using Functional MFnS. After validation of the specificity and sensitivity of the Ab-MFnS nanoplatform in a simple buffer (1X PBS), we proceeded to evaluate the analytical performance of Ab-MFnS in more complex media, including whole blood and PC. These media were selected to mimic a real-world application for our nanosensors, both being shown to be suitable for bacterial growth. Initially, MFnS-S.e. (200 μL, [Fe] = 2 mmol) was added to two serially diluted parallel samples of nutrient-broth-cultured *S. epidermidis* (500 μL, 1−200 CFUs/mL), each containing 200 μL of blood and PC. These solutions were incubated for 15 min at 37 °C and then transferred to a relaxometer tube for T_2 measurements. The MR results from Figure 6A,C demonstrated that lower concentrations (1−50 CFUs/mL) of bacteria yielded dose-dependent changes in the ΔT_2 values, and as expected, the ΔT_2 values showed minimal changes at higher concentrations.

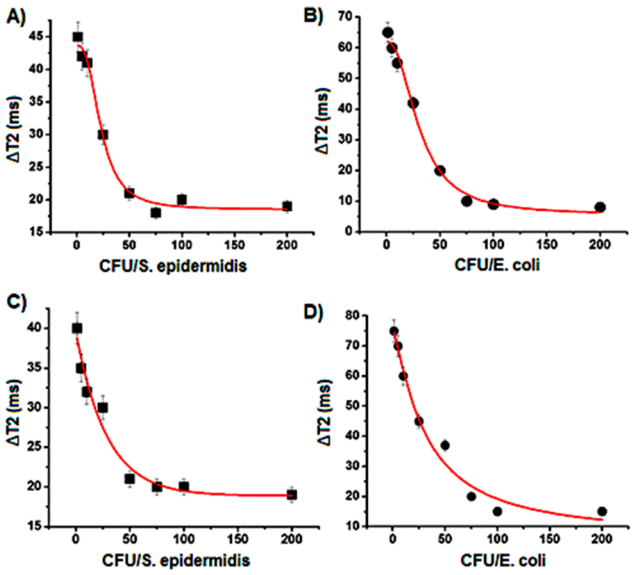

Figure 6. (A and C) *S. epidermidis* and (B and D) *E. coli* cultured in nutrient broth. Specific Ab-MFnS (200 μL, [Fe] = 2 mmol) was added to serially diluted samples (500 μL) of *S. epidermidis* or *E. coli*, each containing 200 μL of blood (A and B) and PC (C and D). After 15 min of incubation at 37 °C, the samples were transferred to a relaxometer tube, and T_2 MR measurements were performed. Each experiment was performed in triplicate, and the data are represented as mean ± standard deviation errors.

Similar results obtained for *E. coli* detection in whole blood and PC using the functional MFnS-E.c., and the results are shown in Figure 6B−D. Overall, the MFnS sensitivity in complex media followed a trend similar to that in the simple buffer. Different parameters are important in the evaluation of effective bacterial detection, including the sample volume, where a larger volume is known to yield more accurate results. However, larger blood sample volumes result in a reduced number of PCs available for transfusion.[6] Therefore, the need for a low level of detection is significant, which can be achieved by the MR mechanism of the proposed MFnS. Our study showed that the binding of MFnS at low pathogen concentrations yielded very sensitive MR signals, as shown in Figure 6.

Simultaneous Detection of Two Target Bacteria Using MFnS. Next, the specificity of our nanosensor was further tested using a MR technique and fluorescence detection in a PC featuring an equal mixture of two pathogens, *S. epidermidis* and *E. coli*. The goal of this experiment was to determine whether our Ab-MFnS could differentiate between two pathogens present in a clinical/environmental sample. To evaluate the multiplex detection capability of MFnS, MFnS-S.e. and MFnS-E.c. were mixed in equal proportions for the simultaneous detection of two bacteria present in a PC. After incubation for 15 min at 37 °C, the solution was transferred to a relaxometer tube, and T_2 measurement was performed. As seen from Figure 7A, the presence of a bacterial mixture leads

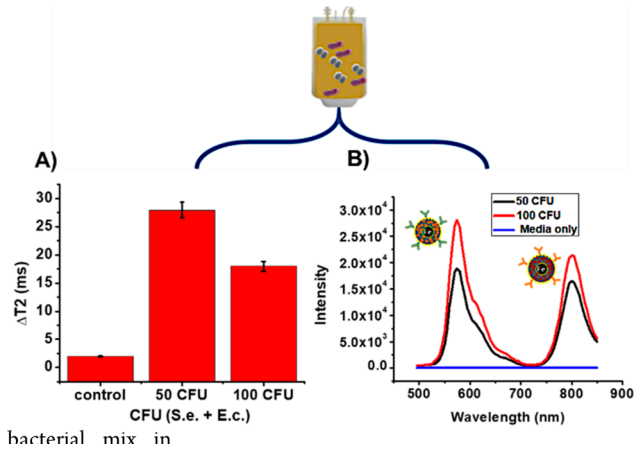

Figure 7. (A) Magnetic relaxation ΔT_2 data for different concentrations of a bacterial mixture in PC. Control: no spiked bacteria in PBS ($\Delta T_2 = \pm 2$). (B) Fluorescence spectra measured from 500 to 850 nm for the simultaneous detection of two bacteria in PCs, *S. epidermidis* (λ_{DiI} = 575 nm) and *E. coli* (λ_{DiR} = 796 nm).

to an average T_2 signal for both the low and higher bacterial counts and, hence, cannot be precisely used to discriminate between two pathogens. Interestingly, fluorescence spectra were measured from suspension of the bacterial cell pellet (procedure as previously described), and two distinct fluorescence emission spectra were obtained for *S. epidermidis* (DiI: λ_{max} = 575 nm) and *E. coli* (DiR: λ_{max} = 796 nm). This is demonstrated for the detection of both contaminants in one step (Figure 7B). As seen, two different concentrations of bacterial solutions were also tested and can be precisely used to discriminate between two pathogens. Control experiments were also performed with no spiked bacteria and media only.

DOI: 10.1021/acsanm.9b01158
ACS Appl. Nano Mater. 2019, 2, 5587−5593

Rapid Assessment of Growth Kinetics of Bacteria Using MFnS. Finally, the assessment of growth kinetics of *S. epidermidis* and *E. coli* was carried out as a validation test for our functional MFnS. In order to reduce and prevent platelet-associated bacterial sepsis, it is important to detect both fast and slow growth kinetics of bacteria. To accomplish this, specific Ab-MFnS (200 μL, [Fe] = 2 mmol) were mixed with 400 μL of a bacterial growth medium (BBL fluid thioglycollate medium) containing 400 μL of PC, with the final concentration of spiked bacteria adjusted to 10 CFUs/mL. This was then incubated at 37 °C for 48 h, and at every 4 h of incubation, T_2 MR data were collected. As shown in Figure 8, PCs contaminated with *S. epidermidis* showed slower growth than those with *E. coli*, and significant bacterial proliferation was observed for *E. coli* between 10 and 12 h. These results demonstrated that our MFnS is also able to distinguish and define *S. epidermidis* as a slow-growing pathogen, while showing *E. coli* proliferating at a much faster rate. This is an important tool because platelet storage usually does not exceed 96 h,[5] limiting both the culture times and potentially bacterial counts to levels below 10 CFUs/mL,[6] which could be even lower especially for slow-growing bacteria such as *S. epidermidis*.

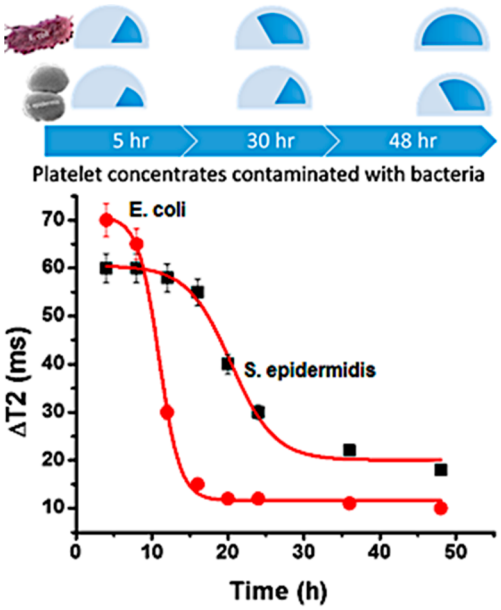

Figure 8. Growth kinetics: 200 μL of specific Ab-MFnS ([Fe] = 2 mmol) incubated with 0.5 mL of PC containing 0.5 mL of a bacterial growth medium (BBL fluid thioglycollate medium), with the final concentration of spiked bacteria adjusted to 10 CFUs/mL at 37 °C for 48 h. At every 4 h of incubation, ΔMR was analyzed. Each experiment was performed in triplicate, and the data are represented as mean ± standard deviation errors.

CONCLUSIONS

In summary, we have generated a multimodal nanosensor platform that can simultaneously screen and identify multiple pathogenic bacteria in a simple buffer system and complex media. The paired techniques of MR and fluorescence complement one another, providing a powerful tool for the rapid detection of bacterial contamination as low as 1 CFU. This nanosensor system also demonstrated the capability of discriminating between two pathogenic bacteria including *E. coli* and *S. epidermidis*. Importantly, cross-reactivity tests established the specificity of MFnS-based detection. Furthermore, a comparison of the analytical performance of MFnS in complex samples including whole blood and PCs with that of a simple buffer revealed that the sensitivity was not compromised, and similar detection limits were achieved in each case. Our multifunctional MFnS has demonstrated the potential for the rapid and sensitive detection of blood-borne pathogens. Additionally, time-dependent assays performed for low concentrations of *E. coli* and *S. epidermidis* further confirmed the sensitivity of MFnS detection. Likewise, our nanosensor system was able to distinguish and identify the characteristically fast and slow growth kinetics of each bacteria, an important aid in the accurate detection and treatment of bacteremia. Taken together, our multimodal MFnS can greatly enhance the ability to detect contaminants in blood products in the early stages, which would markedly improve patient mortality rates. Moreover, this nanosensor technology would significantly aid physicians and care providers for the prompt identification of pathogens, improving therapy and reducing factors responsible for antibiotic-resistant bacteria.

ASSOCIATED CONTENT

Supporting Information

The Supporting Information is available free of charge on the ACS Publications website at DOI: 10.1021/acsanm.9b01158.

Synthesis and characterizations of IONPs, functional MFnS, and supporting characterization data including hydrodynamic diameter, ζ-potential, stability, fluorescence, and MR experiments, as described in the text (PDF)

AUTHOR INFORMATION

Corresponding Authors

*E-mail: tbanerjee@pittstate.edu (T.B.). Tel: 620-235-4749.
*E-mail: ssantra@pittstate.edu (S.S.). Tel: 620-235-4861. Fax: 620-235-4003.

ORCID

Santimukul Santra: 0000-0002-5047-5245

Author Contributions

The project was designed by S.S. and T.B. The experiments were performed by T.T., T.B., W.B., L.H., V.J., and R.E., and the manuscript was written by S.S., T.B., and R.E. All authors have given approval to the final version of the manuscript.

Notes

The authors declare no competing financial interest.

ACKNOWLEDGMENTS

This work is supported by grants to both S.S. and T.B. from the National Institute of Health (Grant 1 R03 AI132832-01) and U.S. Department of Agriculture (Grant SEED 2018-07295) and K-INBRE Bridging Grant P20GM103418 to S.S. We thank Dr. Peter Chung, Department of Biology, Pittsburg State University, for providing bacterial culture facilities.

REFERENCES

(1) Brecher, M. E.; Hay, S. N. Bacterial contamination of blood components. *Clin. Microbiol. Rev.* **2005**, *18*, 195−204.

(2) Brecher, M. E.; Holland, P. V.; Pineda, A. A.; Tegtmeier, G. E.; Yomtovian, R. Growth of bacteria in inoculated platelets: implications for bacteria detection and the extension of platelet storage. *Transfusion* **2000**, *40*, 1308−1312.

DOI: 10.1021/acsanm.9b01158
ACS Appl. Nano Mater. 2019, 2, 5587−5593

(3) Dodd, R. Y. Current viral risks of blood and blood products. *Ann. Med.* **2000**, *32*, 469−474.
(4) Dodd, R. Y. Bacterial contamination and transfusion safety: experience in the United States. *Transfus. Clin. Biol.* **2003**, *10*, 6−9.
(5) CDC, Bacterial Contamination of Platelets. Available from https://www.cdc.gov/bloodsafety/bbp/bacterial-contamination-of-platelets.html (accessed Feb 4, 2019).
(6) Dumont, L. J.; Kleinman, S.; Murphy, J. R.; Lippincott, R.; Schuyler, R.; Houghton, J.; Metzel, P. Screening of single-donor apheresis platelets for bacterial contamination: the passport study results. *Transfusion* **2010**, *50*, 589−599.
(7) Otto, M. Staphylococcus epidermidis-the 'accidental' pathogen. *Nat. Rev. Microbiol.* **2009**, *7*, 555−567.
(8) Lee, H. R.; Seo, J. W.; Kim, M. J.; Song, S. H.; Park, K. U.; Song, J.; Han, K. S. Rapid detection of bacterial contamination of platelet-rich-plasma-derived platelet concentrates using flow cytometry. *Ann. Clin. Lab Sci.* **2012**, *42*, 174−181.
(9) Vollmer, T.; Hinse, D.; Kleesiek, K.; Dreier, J. The Pan Genera Detection immunoassay: a novel point-of-issue method for detection of bacterial contaminants in platelet concentrates. *J. Clin. Microbiol.* **2010**, *48*, 3475−3481.
(10) Muller, T. H.; Mohr, H.; Montag, T. Methods for the detection of bacterial contamination in blood products. *Clin. Chem. Lab. Med.* **2008**, *46*, 933−946.
(11) Davis, T. E.; Fuller, D. D. Direct identification of bacterial isolates in blood cultures using DNA probe. *J. Clin. Microbiol.* **1991**, *29*, 2193−2196.
(12) Tsalik, E. L.; Jones, D.; Nicholson, B.; Waring, L.; Liesenfeld, O.; Park, L. P.; Glickman, S. W.; Caram, L. B.; Langley, R. G.; van Velkinburgh, J. C.; Cairns, C. B.; Rivers, C. P.; Otero, R. M.; Kingsmore, S. F.; Lalani, T.; Fowler, V. G.; Woods, C. W. Multiplex PCR to diagnose Bloodstream infections in Patients Admitted from Emergency Department with Sepsis. *J. Clin. Microbiol.* **2010**, *48*, 26−33.
(13) Mohammadi, T.; Reesink, H. W.; Vandenbroucke-Grauls, C. M.; Savelkoul, P. H. Optimization of Real-Time PCR Assay for Rapid and Sensitive Detection of Eubacterial 16S Ribosomal DNA in Platelet Concentrates. *J. Clin. Microbiol.* **2003**, *41*, 4796−4798.
(14) Dreier, J.; Vollmer, T.; Kleesiek, K. Novel Flow Cytometry-Based Screening for Bacterial Contamination of Donor Platelet Preparations Compared with Other Rapid Screening Methods. *Clin. Chem.* **2009**, *55*, 1492−1502.
(15) Paolucci, M.; Landini, M. P.; Sambri, V. Conventional and molecular techniques for the early diagnosis of bacteraemia. *Int. J. Antimicrob. Agents* **2010**, *36*, S6−S16.
(16) Kempf, V. A.; Mandle, T.; Schumacher, U.; Schafer, A.; Autenrieth, I. B. Rapid detection and identification of pathogens in blood cultures by fluorescence in situ hybridization and flow cytometry. *Int. J. Med. Microbiol.* **2005**, *295*, 47−55.
(17) Johnson, P.; Moriwaki, M.; Johnson, J. Rapid, sensitive detection of bacteria in platelet samples with Fountain Flow Cytometry. *J. Clin. Lab. Anal.* **2017**, *31*, 1−7.
(18) Vollmer, T.; Knabbe, C.; Dreier, J. Novel flow cytometric screeningmethod for bacterial contamination of red blood cells: a proof-of-principle evaluation. *Transfusion* **2014**, *54*, 900−909.
(19) Rood, I. G.; Pettersson, A.; Savelkoul, P. H.; de Korte, D. Performance and suitability of polymerase chain reaction for early detection of bacteria in platelet concentrates. *Transfusion* **2011**, *51*, 2006−2011.
(20) Shao, H.; Min, C.; Issadore, D.; Liong, M.; Yoon, T. J.; Weissleder, R.; Lee, H. Magnetic Nanoparticles and microNMR for Diagnostic Applications. *Theranostics* **2012**, *2*, 55−65.
(21) Haun, J. B.; Yoon, T. J.; Lee, H.; Weissleder, R. Molecular detection of biomarkers and cells using magnetic nanoparticles and diagnostic magnetic resonance. *Methods Mol. Biol.* **2011**, *726*, 33−49.
(22) Kaittanis, C.; Naser, S. A.; Perez, J. M. One-step, Nanoparticle-Mediated Bacterial Detection with Magnetic Relaxation. *Nano Lett.* **2007**, *7*, 380−383.
(23) Chen, Y.; Xianyu, Y.; Wang, Y.; Zhang, X.; Cha, R.; Sun, J.; Jiang, X. One-step detection of pathogens and viruses: combining magnetic relaxation switching and magnetic separation. *ACS Nano* **2015**, *9*, 3184−3191.
(24) Shelby, T.; Banerjee, T.; Kallu, J.; Sulthana, S.; Zegar, I.; Santra, S. Novel magnetic relaxation nanosensors: an unparalleled "spin" on influenza diagnosis. *Nanoscale* **2016**, *8*, 19605−19613.
(25) Shelby, T.; Sulthana, S.; McAfee, J.; Banerjee, T.; Santra, S. Foodborne Pathogen Screening Using Magneto-Fluorescent Nanosensor: Rapid Detection of E.coli O157:H7. *J. Visualized Exp.* **2017**, *127*, 1−7.
(26) Banerjee, T.; Sulthana, S.; Shelby, T.; Heckert, B.; Jewell, J.; Woody, K.; Karimnia, V.; McAfee, J.; Santra, S. Multiparametric Magneto-fluorescent Nanosensors for the Ultrasenitive Detection of Escherichia coli O157:H7. *ACS Infect. Dis.* **2016**, *2*, 667−673.
(27) Santra, S.; Kaittanis, C.; Grimm, J.; Perez, J. M. Drug/Dye-Loaded, Multifunctional Iron oxide Nanoparticles for Combined Targeted Cancer Therapy and Dual Optical/Magnetic Resonance Imaging. *Small* **2009**, *5*, 1862−1868.

DOI: 10.1021/acsanm.9b01158
ACS Appl. Nano Mater. 2019, 2, 5587−5593